AD-A041 775 OHIO STATE UNIV COLUMBUS ELECTROSCIENCE LAB F/G 20/6
AN IMPROVED FORMULATION FOR EXTENDING THE GEOMETRICAL THEORY OF--ETC(U)
MAY 77 J SAHALOS, G A THIELE N00014-76-C-0573
UNCLASSIFIED ESL-4372-2 NL

1 OF 1
AD A041775

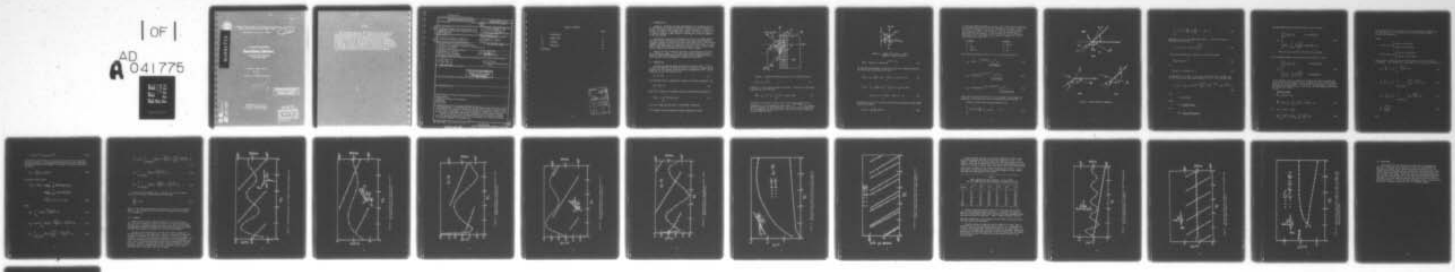

END

DATE FILMED
8-77

AN IMPROVED FORMULATION FOR EXTENDING THE GEOMETRICAL THEORY OF DIFFRACTION BY THE MOMENT METHOD

John Sahalos and Gary A. Thiele

The Ohio State University

ElectroScience Laboratory

Department of Electrical Engineering
Columbus, Ohio 43212

Technical Report 4372-2

May 1977

Contract No. N00014-76-C-0573

UNCLASSIFIED

SECURITY CLASSIFICATION OF THIS PAGE (When Data Entered)

REPORT DOCUMENTATION PAGE

READ INSTRUCTIONS BEFORE COMPLETING FORM

1 REPORT NUMBER

2. GOVT ACCESSION NO.

3 RECIPIENT'S CATALOG NUMBER

4. TITLE (and Subtitle)

AN IMPROVED FORMULATION FOR EXTENDING THE GEOMETRICAL THEORY OF DIFFRACTION BY THE MOMENT METHOD,

5. TYPE OF REPORT & PERIOD COVERED

Technical Report,

6 PERFORMING ORG. REPORT NUMBER

ESL-4372-2

7. AUTHOR(s)

John Sahalos and Gary A. Thiele

8. CONTRACT OR GRANT NUMBER(s)

N00014-76-C-0573

9. PERFORMING ORGANIZATION NAME AND ADDRESS

The Ohio State University ElectroScience Laboratory, Department of Electrical Engineering, Columbus, Ohio 43212

10 PROGRAM ELEMENT, PROJECT, TASK AREA & WORK UNIT NUMBERS

11. CONTROLLING OFFICE NAME AND ADDRESS

Department of the Navy
Office of Naval Research
Arlington, Virginia 22217

12. REPORT DATE

May 1977

13. NUMBER OF PAGES

23

14. MONITORING AGENCY NAME & ADDRESS (if different from Controlling Office)

12 27 p.

15. SECURITY CLASS. (of this report)

Unclassified

15a. DECLASSIFICATION/DOWNGRADING SCHEDULE

16. DISTRIBUTION STATEMENT (of this Report)

DISTRIBUTION STATEMENT A
Approved for public release;
Distribution Unlimited

17. DISTRIBUTION STATEMENT (of the abstract entered in Block 20, if different from Report)

18. SUPPLEMENTARY NOTES

19. KEY WORDS (Continue on reverse side if necessary and identify by block number)

Moment Method
Geometrical Theory of Diffraction
Scattering
Diffraction

20. ABSTRACT (Continue on reverse side if necessary and identify by block number)

Previous work in extending the GTD via the moment method required special consideration for those cases where the incident ray was nearly tangent to one of the faces of the wedge. This difficulty may be overcome by using a series of three terms based upon approximate expressions for the Fresnel integral.

Results are shown for the currents on the faces of a wedge calculated with the improved formulation and these are compared with the exact results. In all cases agreement is excellent.

DD FORM 1 JAN 73 1473 EDITION OF 1 NOV 65 IS OBSOLETE

UNCLASSIFIED

SECURITY CLASSIFICATION OF THIS PAGE (When Data Entered)

402 251

TABLE OF CONTENTS

		Page
I.	INTRODUCTION	1
II.	FORMULATION	1
III.	EXAMPLES	10
IV.	CONCLUSION	22
REFERENCES		23

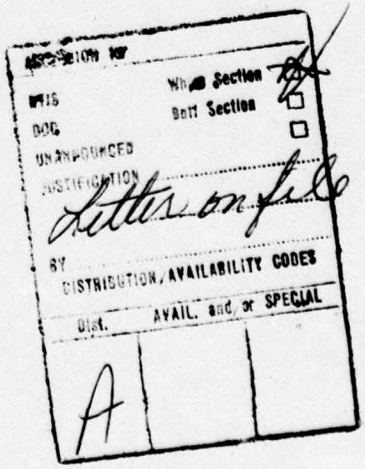

I. INTRODUCTION

Recently a technique has been developed [1] for extending the use of the Geometrical Theory of Diffraction (GTD) by using the method of moments to represent the current near a discontinuity in a surface such as near the edge of a two dimensional wedge. The wedge, of course, is a canonical problem in the GTD and is used merely as a basic geometry to test the method.

The previous work [1] in extending the GTD via the moment method required special consideration for those cases where the incident ray was nearly tangent to one of the faces of the wedge and the results were somewhat dependent upon the location of the match points used. In this report these difficulties are overcome by using a series of three terms based on approximate expressions for the Fresnel integral.

Results for the currents on the faces of the wedge will be shown for a variety of cases. In all cases the currents obtained by the improved combined GTD moment method formulation are compared with the exact currents and the agreement is found to be excellent.

II. FORMULATION

Consider the general wedge diffraction situation shown in Figure 1. The total magnetic field at any point of the space is given as the summation of the incident field $\vec{H}^i$ and the scattered field $\vec{H}^s$. At the point $P(\rho_1,\phi_1,\theta_1)$ the field will be

$$\vec{H} = \vec{H}^i + \vec{H}^s \tag{1}$$

The scattered field is expressed in terms of the vector potential A by

$$\vec{H}^s = \frac{1}{\mu} \vec{\nabla} \times \vec{A} \tag{2}$$

where $\vec{A}$ is related to the wedge current by the following expression

$$\vec{A}(\rho_1) = \mu \iint_{sw} \vec{J}(\vec{r})\, G(\hat{\rho}_1,\hat{r})\, ds' \tag{3}$$

(sw is the wedge surface and G is the Green's function).

If we suppose that the wedge has perfect conductivity then

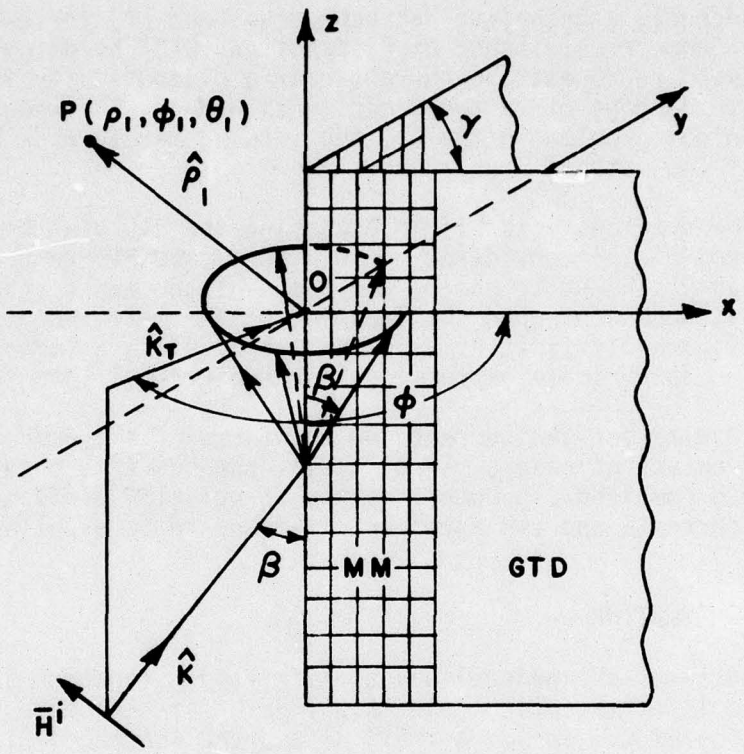

Figure 1. Wedge diffraction geometry used in MM-GTD solution.

$$\vec{J}(\vec{r}) = \hat{n}_r \times \vec{H}(\vec{r}) \tag{4}$$

where $\hat{n}_r$ is a unit vector normal to the wall. By the use of the above equations we can find that:

$$\vec{J}(\vec{r}) = \hat{n}_r \times \vec{H}^i - \hat{n}_r \times \iint_{sw} \vec{J}(\vec{r}') \times \nabla_r G(\hat{r},\hat{r}')ds' \quad . \tag{5}$$

Given that the magnetic field as well as the vector potential are dependent on z only through the phase factor $e^{-jkz\cos\beta_o}$, all problems we will consider are two-dimensional. The current may be represented by the components $\vec{J}_T$ on xy plane and $\vec{J}_z$ on xz or yz plane (Figure 2) and will take the form:

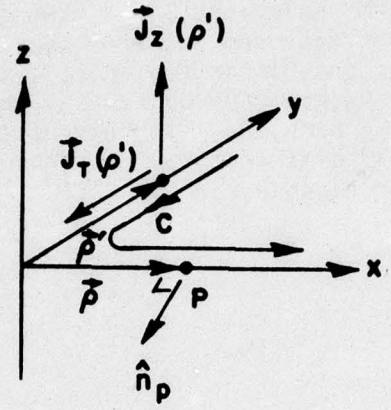

Figure 2. Current of a point ρ' used in magnetic integral equation.

$$\vec{J}(\vec{r}') = [\vec{J}_z(x,y) + \vec{J}_T(x,y)]e^{-jkz\cos\beta_o} \tag{6}$$

By the help of Equations (5) and (6) we have the integral expression for the $\vec{J}_T$ and $\vec{J}_z$ currents as follows:

$$\vec{J}_T(\rho) = \hat{n}_p \times \vec{H}_z^i(\rho) - \hat{n}_p \times \int_c \vec{J}_T(\rho') \times \nabla_p G(\rho,\rho') \cdot d\ell' \tag{7}$$

$$\vec{J}_z(\rho) = \hat{n}_p \times \vec{H}_T^i(\rho) - \hat{n}_p \times \int_c \vec{J}_z(\rho') \times \nabla_p G(\rho,\rho') d\ell' -$$

$$-jk_z \hat{n}_p \times \hat{z} \times \int_c \vec{J}_T(\rho') \cdot G(\rho,\rho') \cdot d\ell' \quad . \tag{8}$$

The Green's function in the two dimensional case reduces to the Hankel function [2] and is

$$G(\rho,\rho') = \frac{1}{4j} H_o^2(k_T|\vec{\rho}-\vec{\rho}'|) \quad . \tag{9}$$

In using the GTD-MM solution [1] we must first recognize the difference in the diffraction near and far from the edge of the wedge. Thus, if the plane of incidence is in region (I), then we have two reflected rays (Figure 3a) R_0, R_1. And we can say that the problem may be separated into two problems. In both of them we have to study the diffraction from 3 different rays as shown in Figures 3b,c. The incident angles for these are:

xz plane	yz plane
1. ϕ	1. $360-\phi-\gamma$
2. $360-\phi$	2. $\phi-\gamma$
3. $360-\phi-2\gamma$	3. $\phi+\gamma$

The diffracted current on the x axis will be the summation of:

$$J_{1x} = D^x(\phi) \cdot e^{-jk_T r\cos\phi} \int_{\sqrt{k_r r(1+\cos\phi)}}^{\infty} e^{-j\tau^2}\, d\tau \tag{10}$$

$$J_{2x} = D^x(360-\phi) e^{jk_T r\cos\phi} \int_{\sqrt{k_r r(1+\cos\phi)}}^{\infty} e^{-j\tau^2}\, d\tau \tag{11}$$

$$J_{3x} = D^x(360-\phi-2\gamma)\, e^{jk_T r\cos(\phi+2\gamma)} \int_{\sqrt{k_r r(1+\cos(\phi+2\gamma))}}^{\infty} e^{-j\tau^2}\, d\tau \tag{12}$$

where the diffraction coefficients D^x are assumed to be unknown and dependent on each other and the corresponding D^y on the y-axis.

A Fresnel integral can be approximated as [3]:

$$\int_{\sqrt{x}}^{\infty} e^{-j\tau^2}\, d\tau \simeq \sqrt{\frac{2}{\pi}}\ (a_0 + a_1\sqrt{x}) , \qquad x \to 0 \tag{13}$$

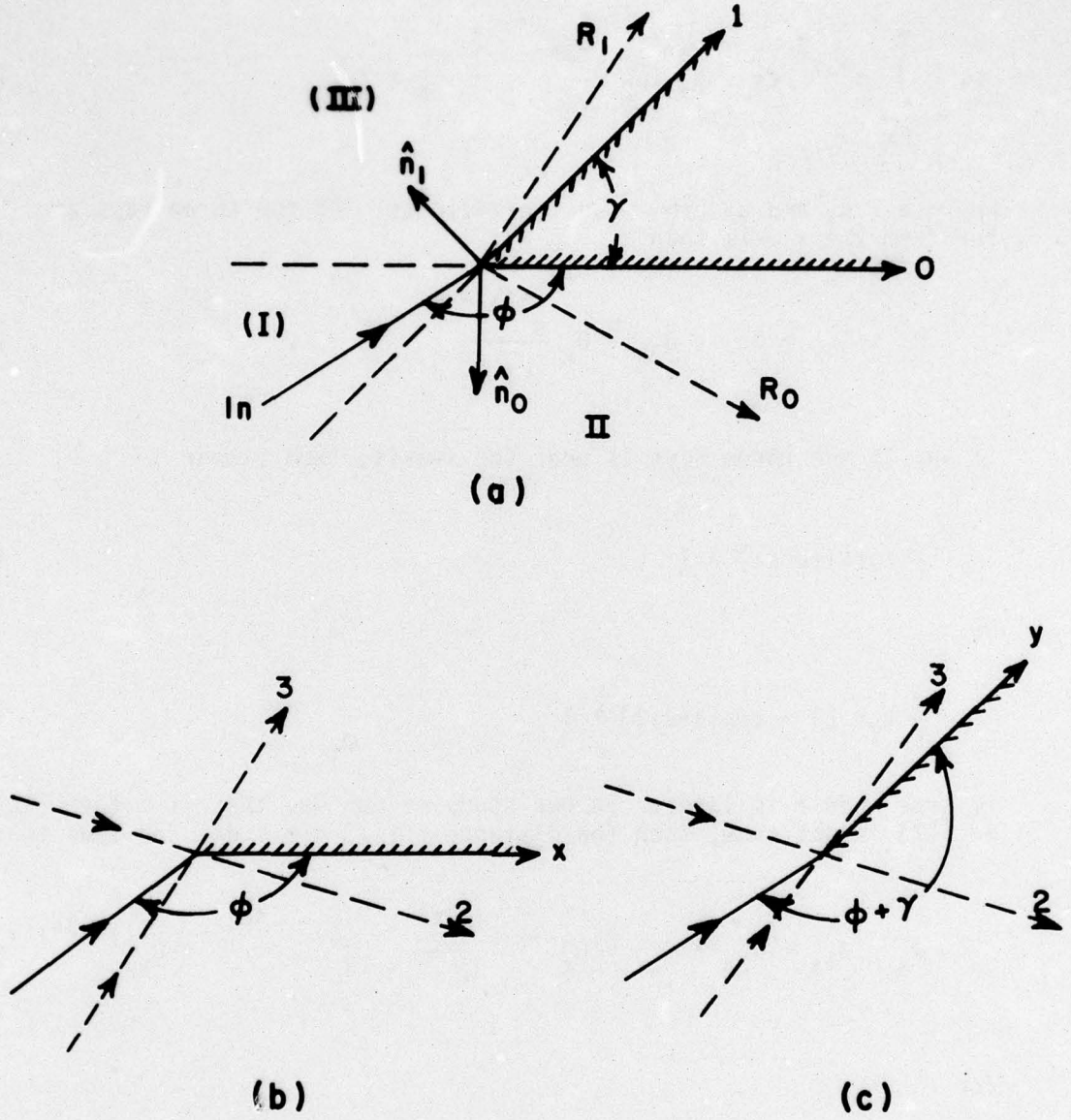

Figure 3. Wedge reflection geometry.

$$\int_{\sqrt{x}}^{\infty} e^{-j\tau^2}\, d\tau \simeq \sqrt{\frac{2}{\pi}}\; a_2\, \frac{e^{-jx}}{\sqrt{x}} \quad , \qquad \frac{2}{\pi}\, x > 1 \tag{14}$$

where a_0, a_1 and a_2 are known coefficients. If the three rays are far from the x axis then

$$J_x = J_{1x} + J_{2x} + J_{3x} \simeq D_x\, \frac{e^{-jk_T x}}{\sqrt{x}} \quad . \tag{15}$$

If any of the three rays is near the x-axis, then either

$$\frac{2}{\pi}\, k_T r(1+\cos\phi) > 1 \tag{16}$$

or

$$\frac{2}{\pi}\, k_T r\, [1 + \cos(\phi+2\gamma)] > 1 \tag{17}$$

is true when r is large. In our study we can say that if either (16) or (17) is not true, then the distance r is $0 < r < 3\lambda$, and thus that

$$J_x = J_{1x} + J_{2x} + J_{3x} \simeq D_x^{(-1)}\, \frac{e^{-jK_T x}}{\sqrt{x}} + D_x^{(0)}\; e^{jk_T x} + D_x^{(1)}\, e^{jk_T x}\, \sqrt{x} \tag{18}$$

for

$$r > \min(r_1^x, r_2^x)$$

where

$$r_1^x = \frac{\lambda}{4\sin\beta_o(1+\cos\phi)}$$

and

$$r_2^x = \frac{\lambda}{4\sin\beta_o[1+\cos(\phi+2\gamma)]} \quad .$$

The approximation of the total current on x-axis will be

$$J_x = \begin{cases} \sum_{n=1}^{k} a_m^x P(x-x_m) & 0<x<\min(r_1^x, r_2^x) \\ J_x^i + J_x^r + \sum_{n=-1}^{1} D_x^n \dfrac{e^{-jk_T x}}{(\sqrt{x})^n} & \min(r_1^x, r_2^x) <x<\infty \end{cases} \tag{19}$$

where $P(x-x_m)$ is a pulse function with a_m^x weight.

The same approximation can be used for the current on y-axis

$$J_y = \begin{cases} \sum_{m=1}^{N} a_m^y P(y-y_m) & 0<y<\min(r_1^y, r_2^y) \\ J_y^i + J_y^r + \sum_{n=-1}^{1} D_y^n \dfrac{e^{-jk_T y}}{\sqrt{y}} & \min(r_1^y, r_2^y)<y<\infty \end{cases} \tag{20}$$

.

If the incident ray is in region (II) (Figure 3a), then in expressions (19), (20) we will not have J^l or J^r in the face which is in the shadow region of the incident plane. By the help of the equation (1) and with the same work as Burnside et al. [1] we can find the unknown coefficients a_m^x, a_m^y, D^x, D^y. Thus,

Point on x-axis

1. MM - region $(x=x_n)$

$$\frac{a_n^x}{2} + \sum a_m^y I_{mn} + \sum_{\ell=-1}^{1} D_y^\ell I_n^\ell = -H_z^i(x_n) - k_n \quad . \tag{21}$$

2. GTD - region $(x=x_D)$

$$\frac{1}{2} \sum_{n=-1}^{n} D_x^n E_x^n + \sum a_m^y I_{m_D} + \sum_{\ell=-1}^{1} D_y^\ell I_D^\ell = -k_D \tag{22}$$

the expression for points on the y-axis can be found by changing the x to y and the y to x. In a general case for finding the unknowns we need k+N+6 equations:

Taking

$$\text{on the x-axis} \begin{cases} k \text{ points on MM region} \\ 3 \text{ points on GTD region} \end{cases}$$

$$\text{and on the y-axis} \begin{cases} N \text{ points on MM region} \\ 3 \text{ points on GTD region} \end{cases}$$

we will have a linear system of k+N+6 equations with an equal number of unknowns. The coefficients in Equations (21) and (22) are of the form:

$$I_{mn} = \frac{k_T}{4j} x_n \sin \int_{\delta y_m}^{\infty} \frac{H_1^2(k_T r)}{r} dy \tag{23}$$

$$I_n^{\ell} = \frac{k_T}{4j} x_n \sin \int_{\min(r_1^y, r_2^y)}^{\infty} \frac{e^{-jk_T y}}{(\sqrt{y})^{\ell}} \frac{H_1^2(k_T r)}{r} dy \tag{24}$$

$$k_n = -\frac{k_T}{2j} x_n \sin\gamma \int_{\min(r_1^y, r_2^y)}^{\infty} H_z^i(y) \frac{H_1^2(k_T r)}{r} dy \tag{25}$$

$$E_x^n = \frac{e^{-jk_T x_D}}{(\sqrt{x_D})^n} \tag{26}$$

and

$$r = [x_n^2 + y^2 - 2x_n y \cos\gamma]^{1/2} \tag{27}$$

Substituting the current J_T in Equation (8) one can find in the same way the J_z current. A more applicable expression for J_z current can be found with the help of Maxwell's Equations from which we can easily show that

$$\vec{J}_z = -j \frac{k_z}{k_T^2} \hat{n}_p \times \nabla_p \vec{H}_z(p) \tag{28}$$

By Equation (28) we have:

$$J_z(x_n) = H_T^2(x_n) - \frac{1}{4\tan\beta_o} \sum_{n=1}^{N} a_m^y [\sin\gamma M_{nm} - k_T I_{nm}] -$$

$$- \frac{1}{4\tan\beta_o} \sum_{\ell=-1}^{1} D_y^{\ell} [\sin\gamma K_n^{\ell} - k_T I_n^{\ell}] +$$

$$+ \frac{\cos\beta_o}{2} [\sin\gamma L_n^1 - K_1 L_n^2] \tag{29}$$

where

$$M_{nm} = \int_{\delta y_m} H_1^2(k_T r) \frac{y^2 - x_n y \cos\gamma}{r^3} dy \tag{30}$$

$$I_{nm} = x_n \sin\gamma \int_{\delta y_m} [H_o^2(k_T r) - \frac{H_1^2(k_T r)}{k_T r}] \cdot \frac{x_n - y\cos\gamma}{r} dy \tag{31}$$

$$k_n^{\ell} = \int_{\min(r_1^y, r_2^y)}^{\infty} H_1^2(k_T r) \frac{e^{-jk_T y}}{(\sqrt{y})^{\ell}} \frac{y^2 - x_n y\cos\gamma}{r^3} dy \tag{32}$$

$$I_n^{\ell} = x_n \sin\gamma \int_{\min(r_1^y, r_2^y)}^{\infty} \left[H_0^2(k_T r) - \frac{H_1^2(k_T r)}{k_T r}\right] \frac{e^{-jk_T y}}{(\sqrt{y})^{\ell}} \frac{x_n + y\cos\gamma}{r}\, dy \tag{33}$$

$$L_n^1 = \int_{\min(r_1^y, r_2^y)}^{\infty} H_1^2(k_T r) \frac{y^2 - x_n y\cos\gamma}{r}\, dy \tag{34}$$

$$L_n^2 = \int_{\min(r_1^y, r_2^y)}^{\infty} \left[H_0^2(k_T r) - \frac{H_1^2(k_T r)}{k_T r}\right] \frac{x_n + y\cos\gamma}{r}\, dy \quad . \tag{35}$$

By the help of Equations (8) or (28) we can find the current parallel to the edge. Both methods must show that:

$$\frac{|J_T^d|}{|J_z^d|} = \tan\beta \tag{36}$$

which is also true from the principles of GTD for arbitrary incidence angles if the incident field is such that the problem is not purely TE or purely TM.

III. EXAMPLES

Numerical results have been obtained for a variety of cases. The first set of results is shown in Figure 4 for the situation where a plane wave is incident normally ($\beta_0=\pi/2$) on the edge of a 90° wedge. The agreement between the GTD-MM results obtained using Equations (21) and (22) and the exact solution [4] is seen to be excellent.

Figures 5 and 6 show results for two cases where a plane wave is incident obliquely on the wedge edge. Again, agreement with the exact solution is excellent for both $J_T(x)$ and $J_z(x)$. In Figures 5 and 6 as well as 4, it was only necessary to use the D^1 term in Equations (19) and (20) although the same results are obtained if all three terms are used. This is what one would expect and is in agreement with previous work [1]. However, to obtain the correct results in Figure 7, it was necessary to use all three terms since the incident rays are near grazing on one or the other faces of the wedge.

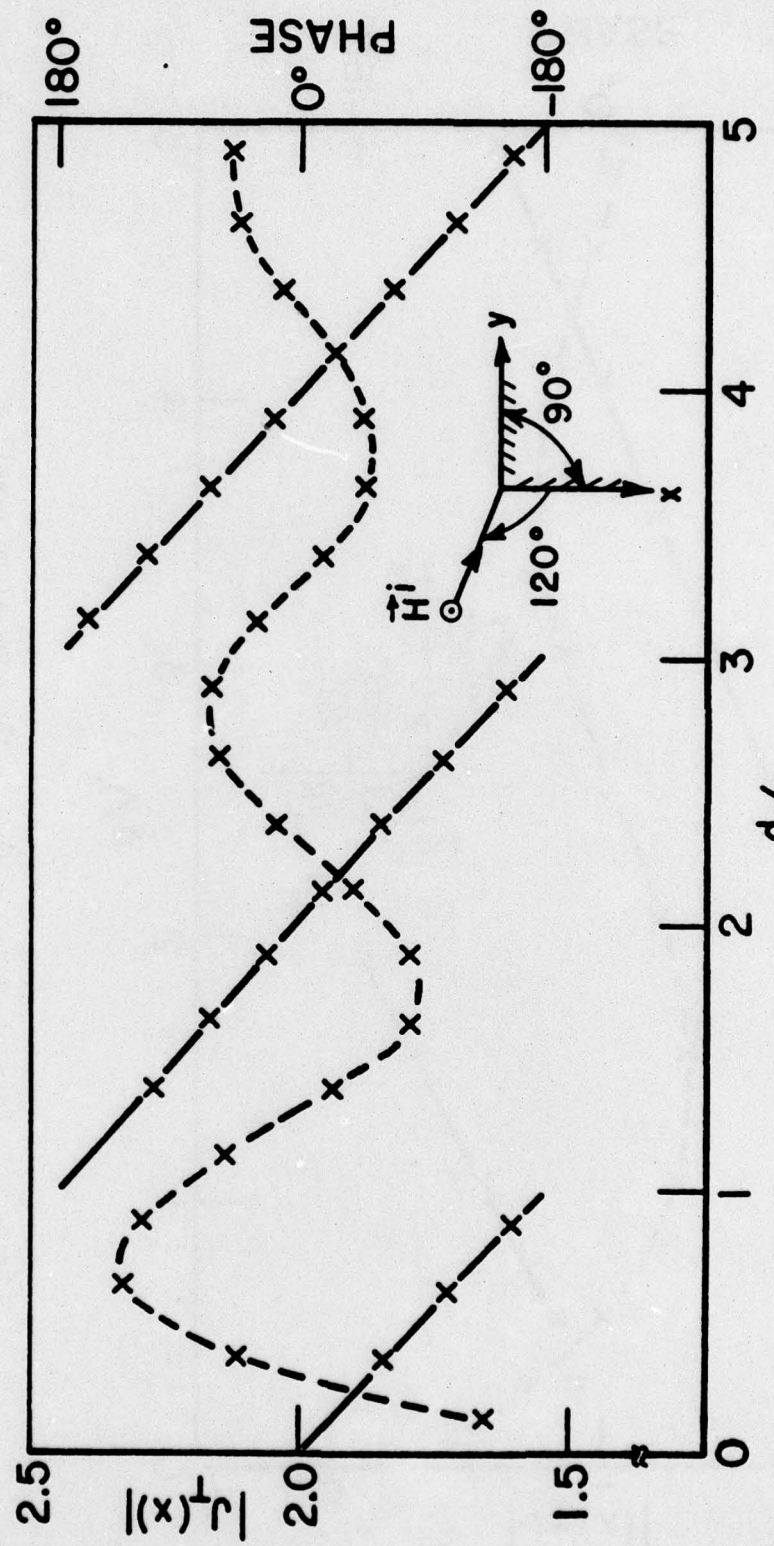

Figure 4. Current along x-wall of 90° wedge for normal incidence case.

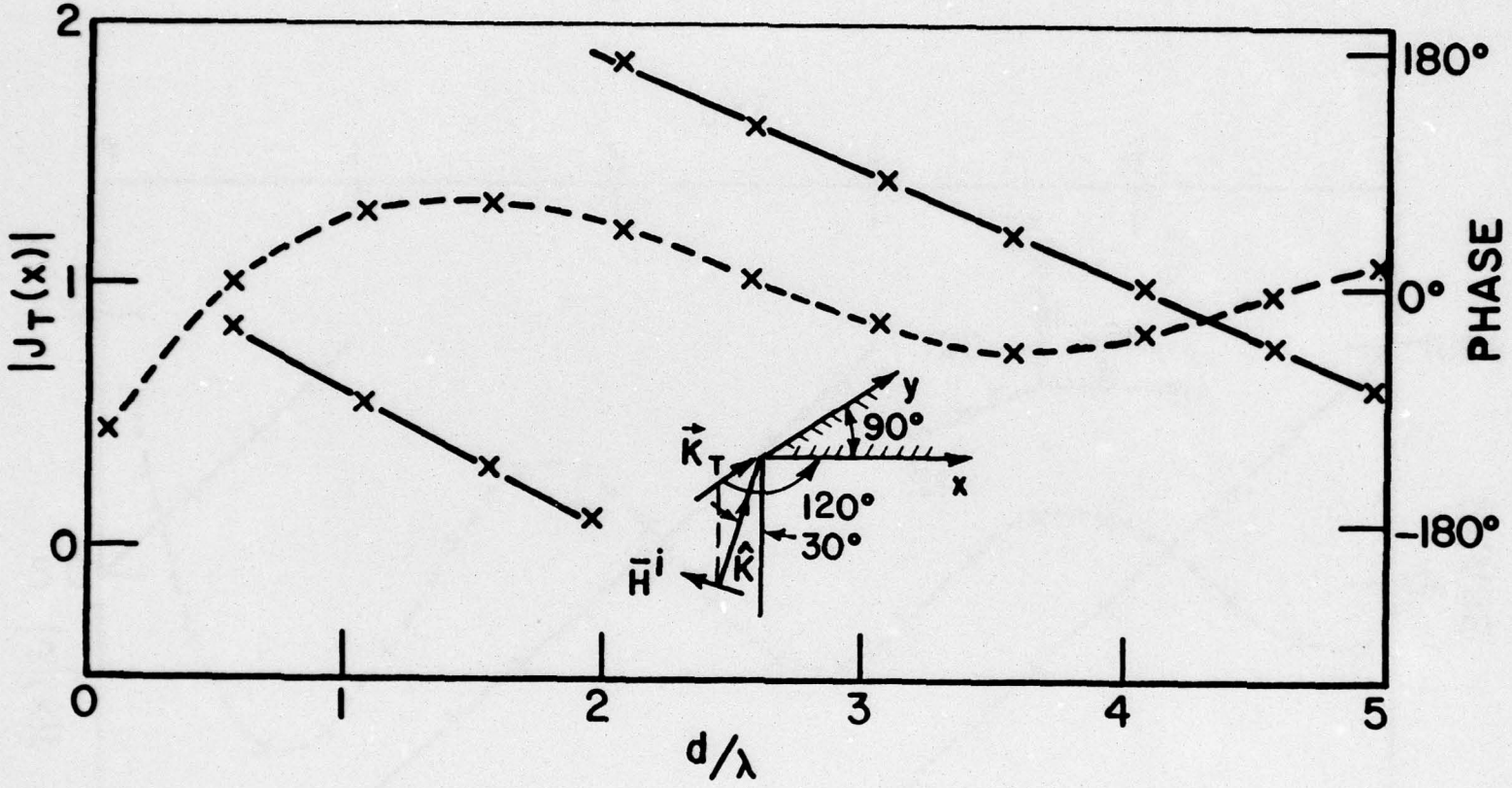

Figure 5a. Current perpendicular to the edge along x-wall of 90° wedge for oblique incidence case.

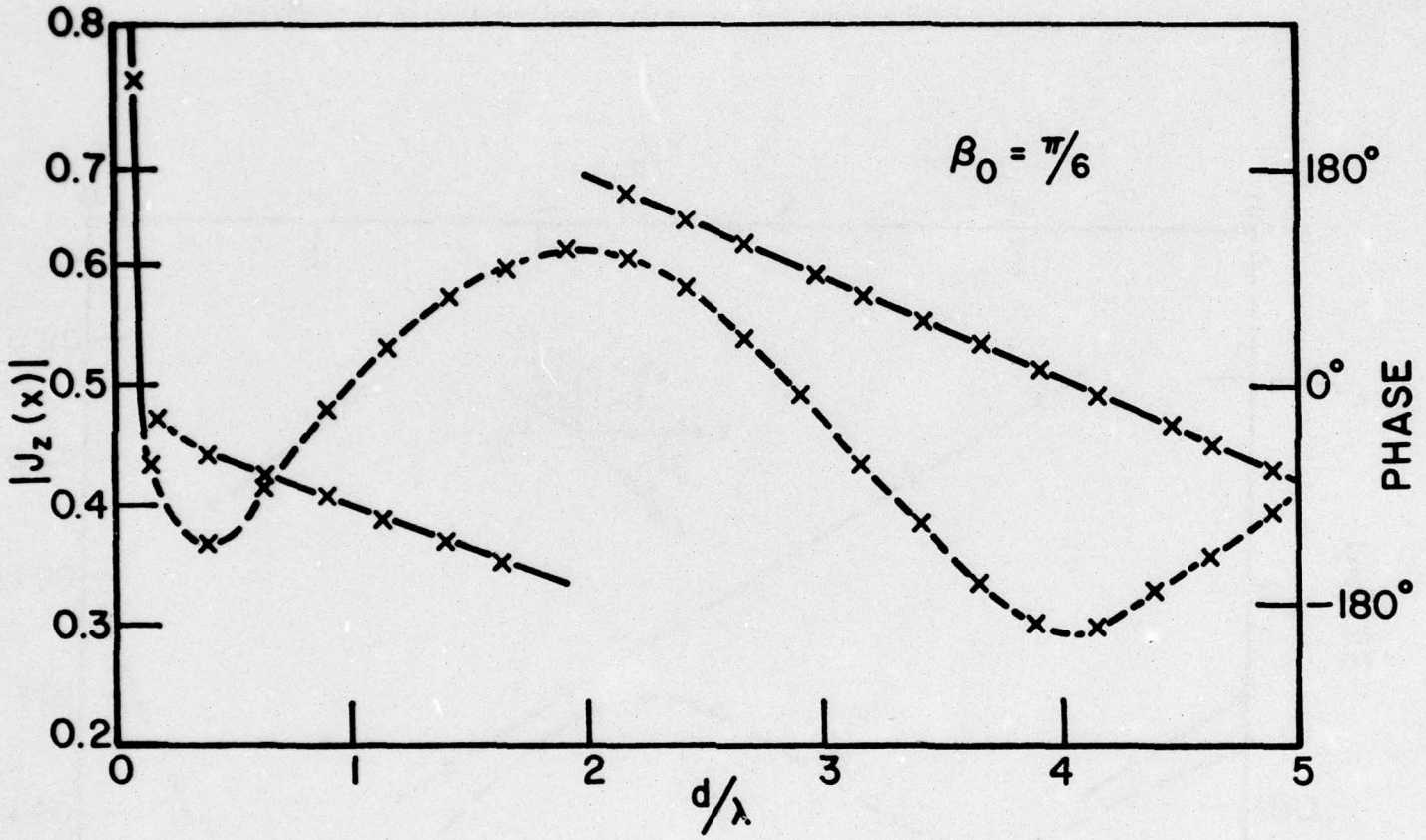

Figure 5b. Current parallel to the edge along x-wall of 90° wedge for oblique incidence case.

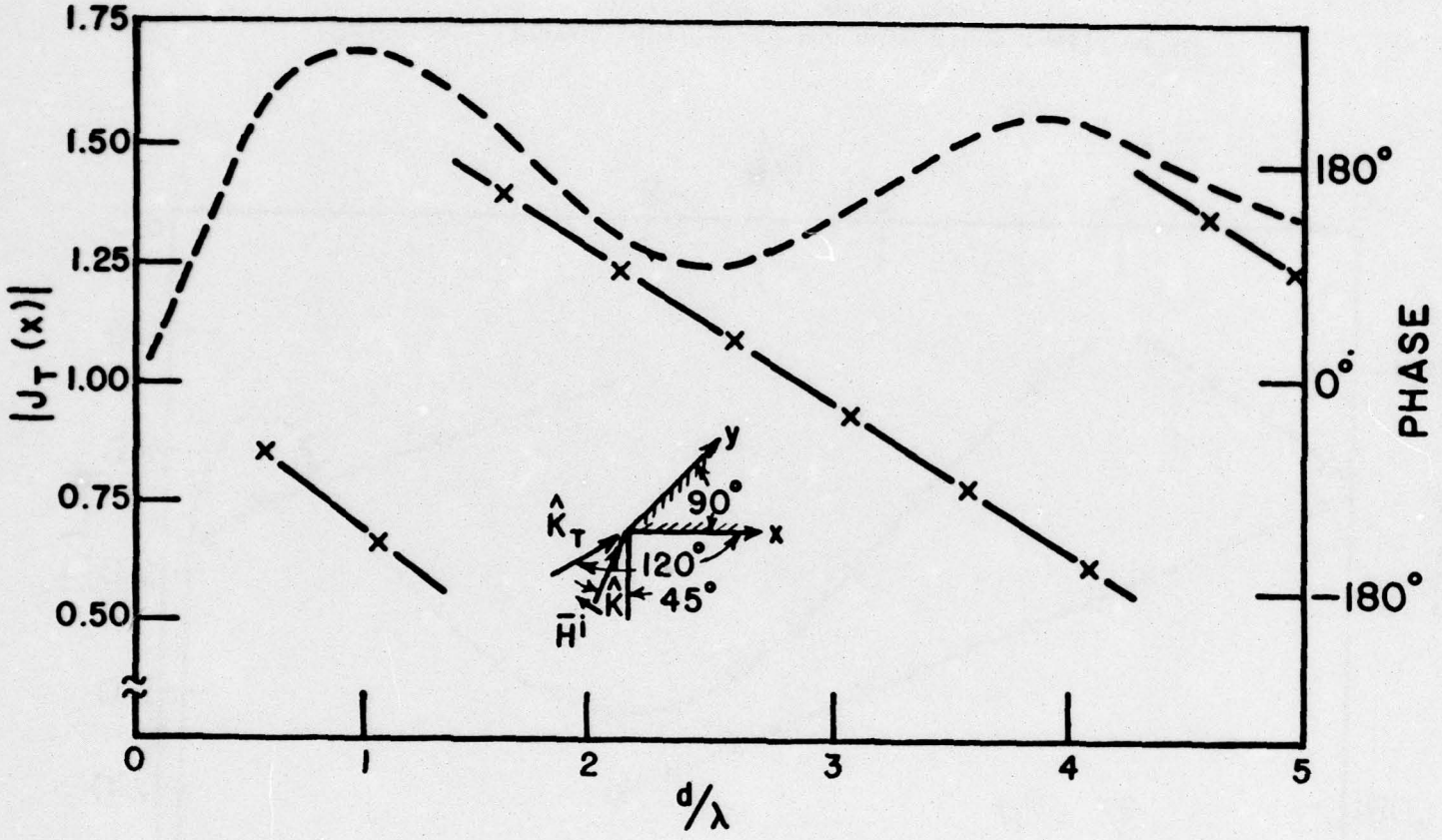

Figure 6a. Current perpendicular to the edge along x-wall of 90° wedge for oblique incidence case.

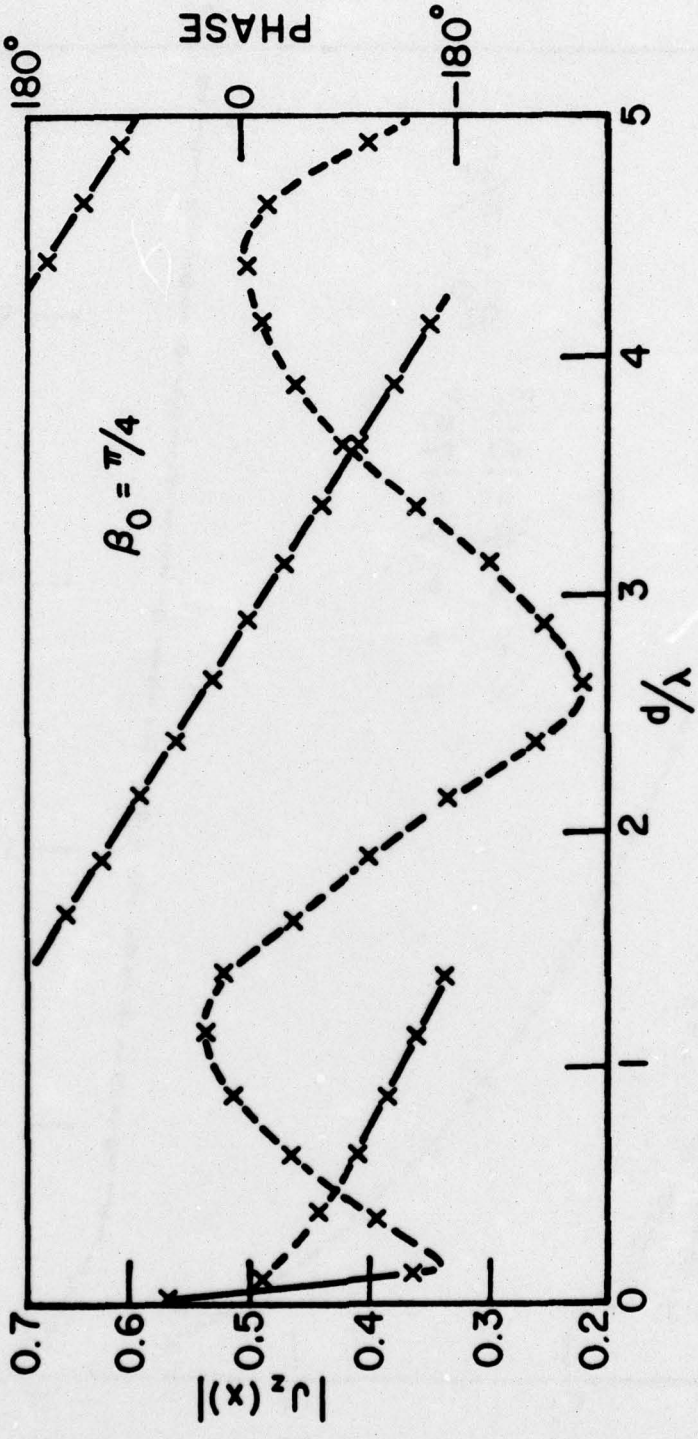

Figure 6b. Current parallel to the edge along x-wall of 90° wedge for oblique incidence case.

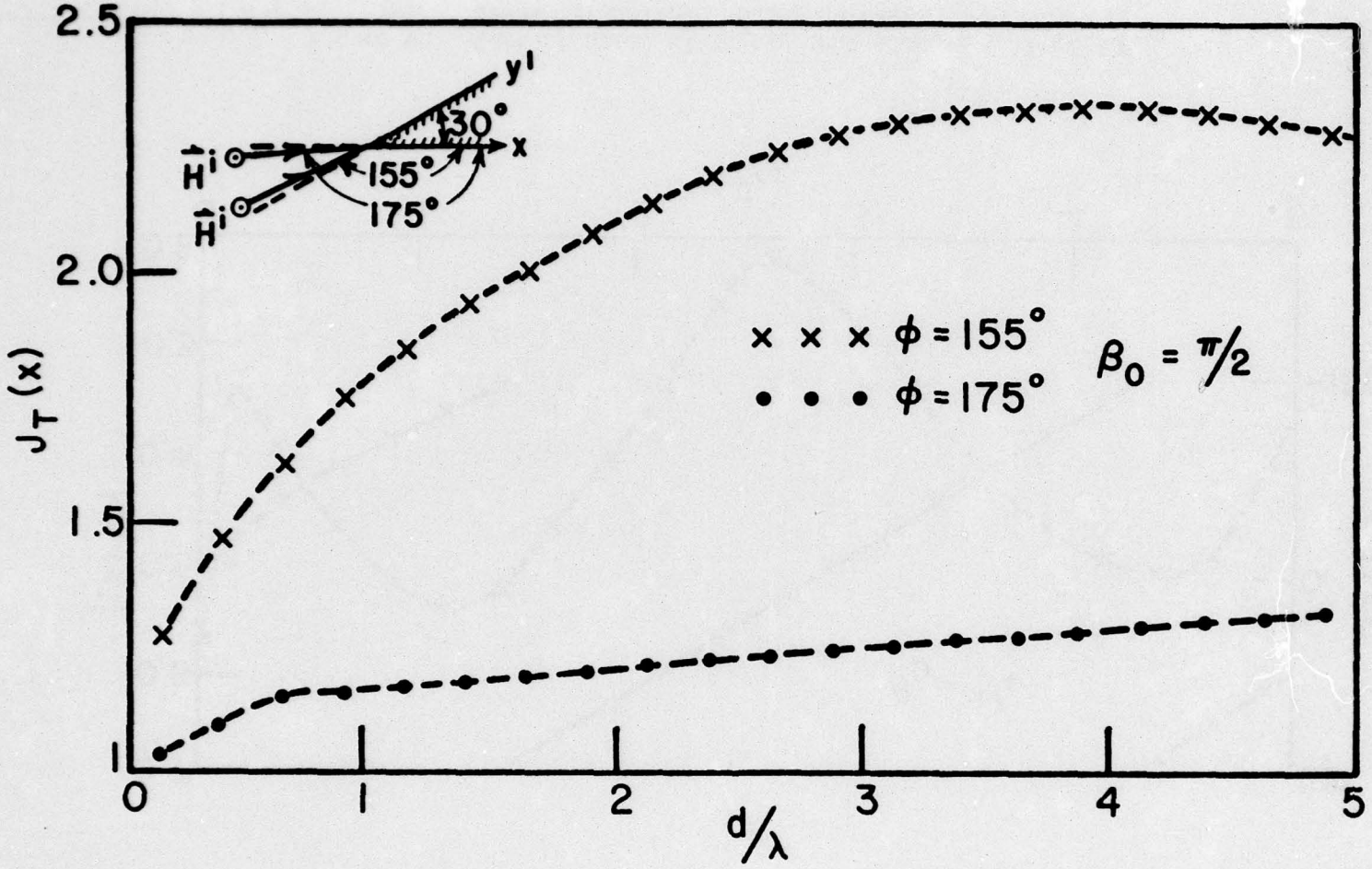

Figure 7a. Magnitude of the currents along x-wall of 30° wedge for two normal incidence cases near the shadow boundaries.

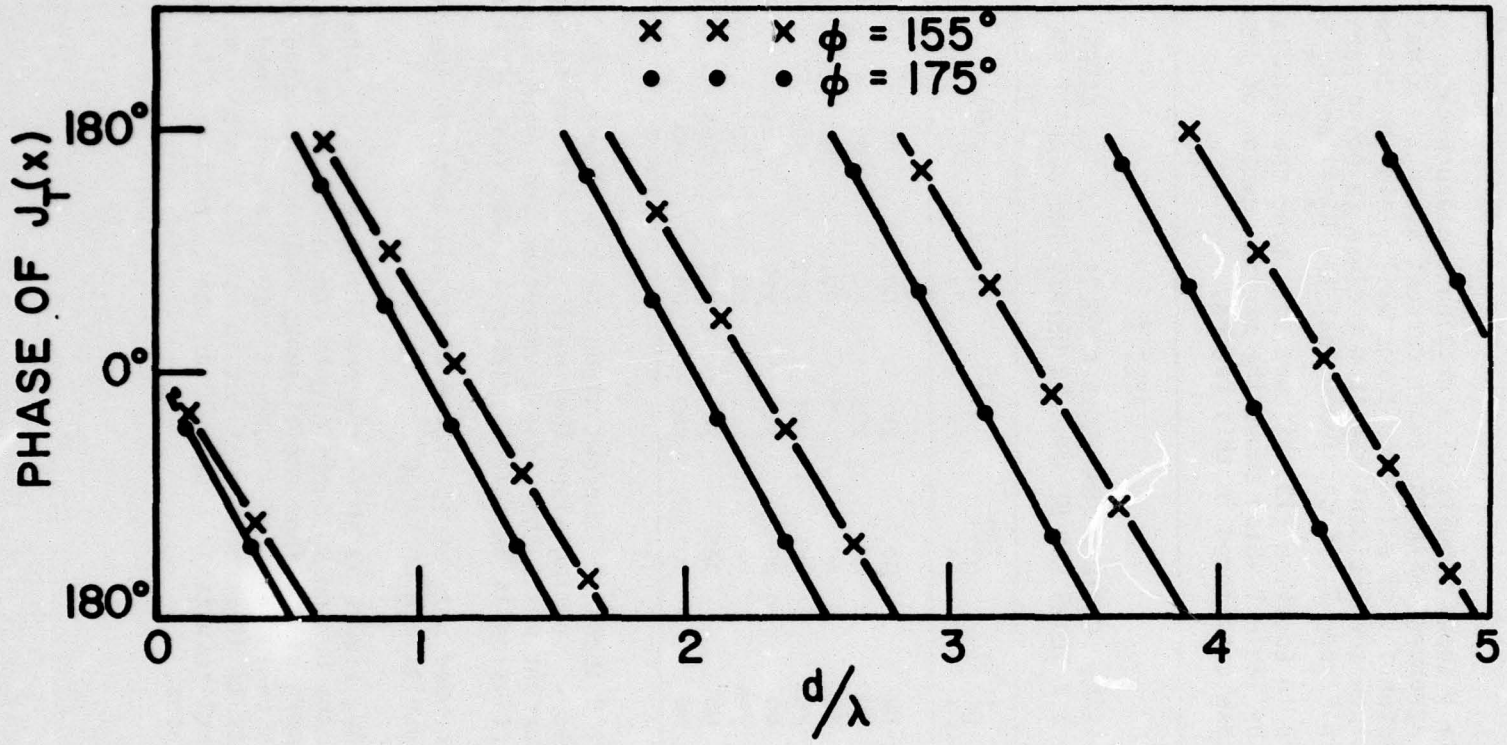

Figure 7b. Phase of the current along x-wall of 30° wedge for two normal incidence cases near the shadow boundaries.

Figure 8 shows results of a grazing incidence case which shows excellent agreement with the exact current along the x wall. As in Figure 7 retention of all three terms will yield the correct results. However, since the incident ray is not close to being parallel to both walls as in Figure 7, it was found that the $D_x^{(-1)}$ and D_x^{0} terms could be set to zero in Equation (19) without effecting the results. This is indicated by Table 1 which shows the minimum number of terms needed for each case considered in this report.

TABLE 1

TERMS REQUIRED FOR VALID RESULTS. IN ALL CASES, ALL SIX TERMS CAN BE USED TO OBTAIN THE CORRECT SOLUTION

Figure	$D_x^{(-1)}$	$D_x^{(0)}$	$D_x^{(1)}$	$D_y^{(-1)}$	$D_y^{(0)}$	$D_y^{(1)}$
4	no	no	yes	no	no	yes
5	no	no	yes	no	no	yes
6	no	no	yes	no	no	yes
7	yes	yes	yes	yes	yes	yes
8	no	no	yes	yes	yes	yes
9	yes	yes	yes	no	no	yes
10a	no	yes	yes	yes	yes	yes
10b	no	no	yes	no	no	yes

Figure 9 shows the current along the x wall when the incident ray is close to grazing along that wall. In contrast to Figure 8, here the current phase shows rapid variation and again agreement with the exact solution is excellent. Table 1 shows that $D_y^{(-1)}$ and $D_y^{(0)}$ need not be used but, as in Figure 8, if all terms in the series are used the results are unchanged.

Finally, Figure 10 shows the results obtained if other combinations of the D_x and D_y coefficients are used. It is apparent that if one or more of the four coefficients required for good results in Figure 9 is excluded, then incorrect results are obtained. Moving the match points to different locations in the GTD region does not affect the incorrect results in Figure 10 or the correct results in the previous cases.

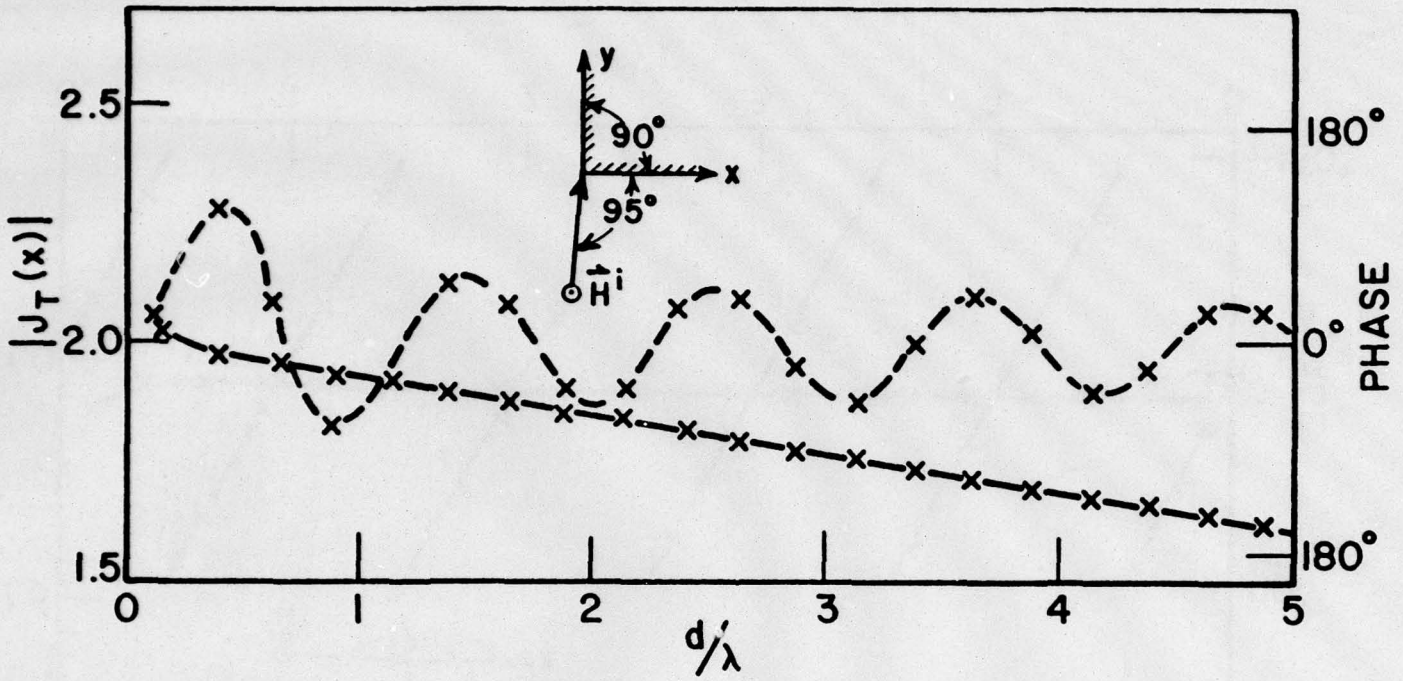

Figure 8. Current along x-wall of 90° wedge for normal incidence case near the shadow boundary of y-wall.

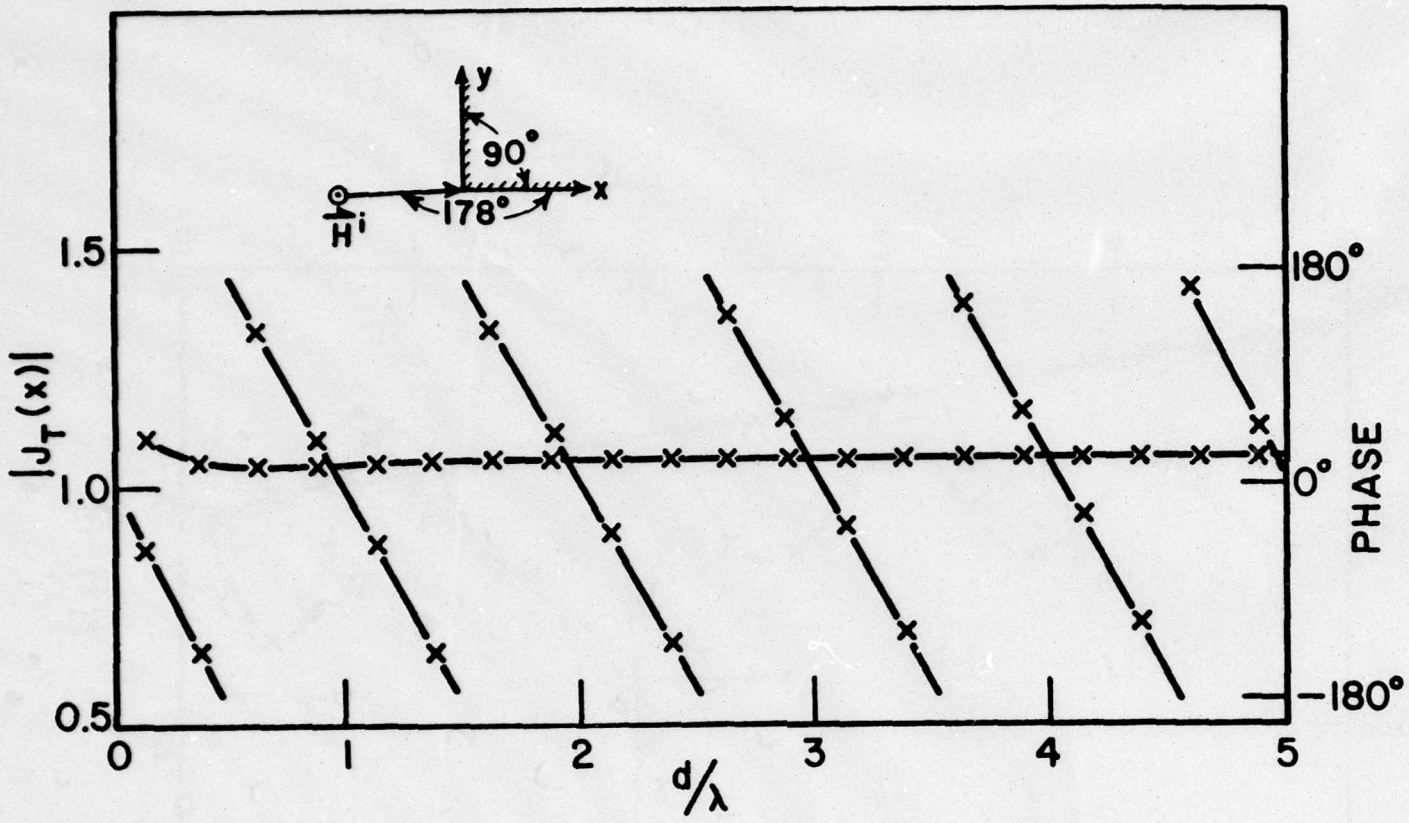

Figure 9. Current along x-wall of 90° wedge for normal incidence case near the shadow boundary of x-wall.

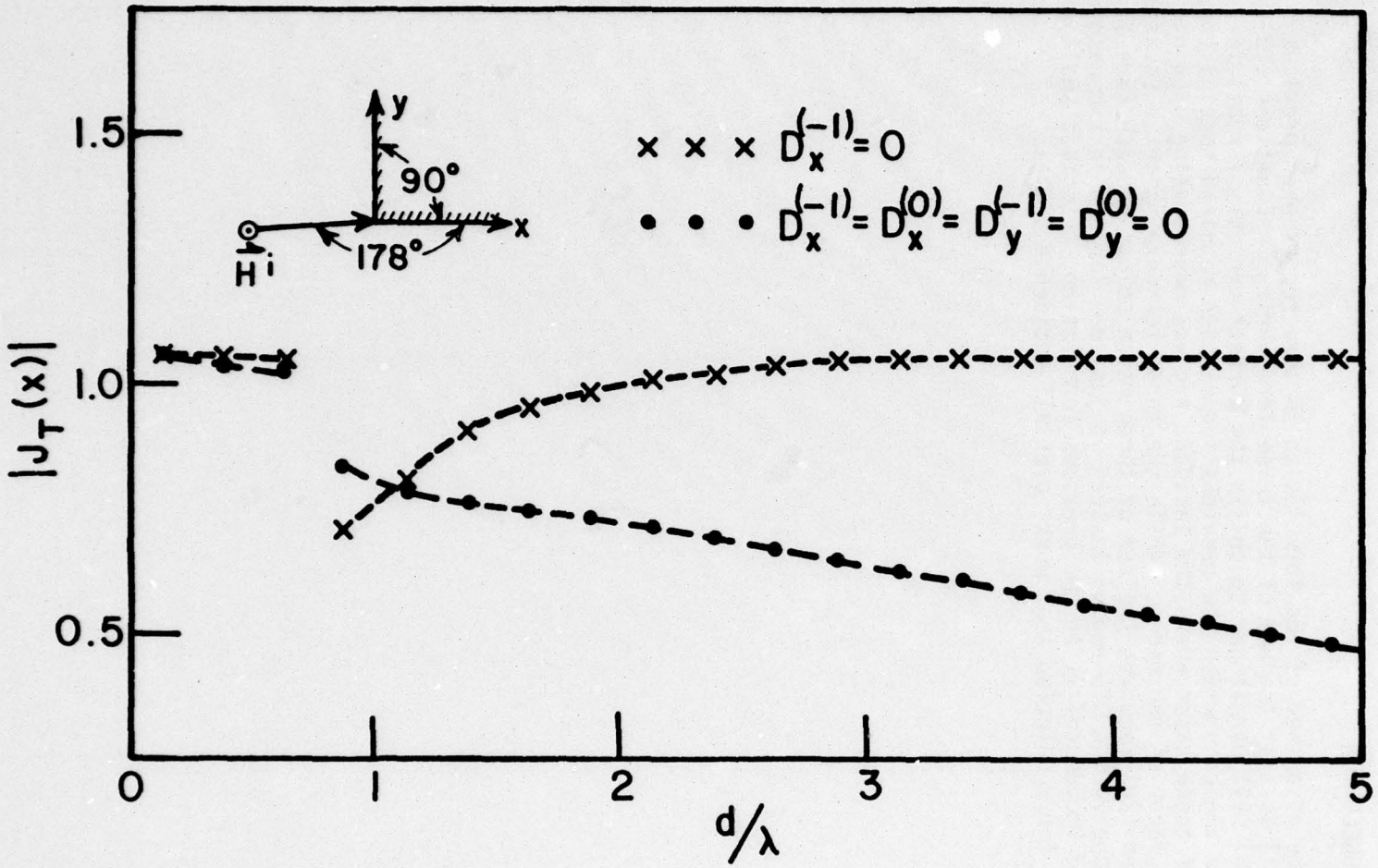

Figure 10. Current along x-wall of 90° wedge for normal incidence case near the shadow boundary of x-wall by using less than three diffraction coefficients.

IV. CONCLUSION

The advantage of the formulation in this report over previous work [1] is that the use of the three term series in Equations (19) and (20) will permit one to obtain the correct currents for all incidence angles whereas the previous formulation required special treatment of those cases where the incident ray was near grazing upon one of the faces of the wedge. While the three term expansion in Equations (19) and (20) requires the use of three match points on each face of the wedge in the GTD region instead of just one (or two in the case of grazing incidence) as in the previous formulation, this is a small price to pay for a solution that works over all incidence angles.

REFERENCES

[1] W. D. Burnside, C. L. Yu, and R. J. Marhefka, "A Technique to Combine the Geometrical Theory of Diffraction and the Moment Method," IEEE Trans. Antennas Propagat., vol. AP-23, pp. 551-558, July 1975.

[2] R. F. Harrington, Field Computation by Moment Methods, New York, MacMillan, 1968.

[3] M. Abramowitz and I. Stegun, Handbook of Mathematical Functions, NBS Applied Mathematics Series No. 55, June 1964.

[4] R. G. Kouyoumjian, "The Geometrical Theory of Diffraction and Its Application," Chapter 6 in Numerical Asymptotic Techniques in Electromagnetics, R. Mittra, Ed., Springer-Verlag, Berlin 1975.